The Plant Cell, Vol. 21: 3641–3654, November 2009, www.plantcell.org © 2009 American Society of Plant Biologists

Control of Cell Proliferation, Organ Growth, and DNA Damage Response Operate Independently of Dephosphorylation of the *Arabidopsis* Cdk1 Homolog CDKA;1 [C][W]

Nico Dissmeyer,[a,b] Annika K. Weimer,[a,b] Stefan Pusch,[a,1] Kristof De Schutter,[c,d] Claire Lessa Alvim Kamei,[c,d] Moritz K. Nowack,[a,2] Bela Novak,[e] Gui-Lan Duan,[f] Yong-Guan Zhu,[f] Lieven De Veylder,[c,d] and Arp Schnittger[a,b,3]

[a] Unigruppe am Max-Planck-Institut für Züchtungsforschung, Max-Delbrück-Laboratorium, Lehrstuhl für Botanik III, Universität zu Köln, D-50829 Köln, Germany

[b] Department of Molecular Mechanisms of Phenotypic Plasticity, Institut de Biologie Moléculaire des Plantes du Centre National de la Recherche Scientifique, Unité Propre de Recherche 2357, Université de Strasbourg, F-67084 Strasbourg Cedex, France

[c] Department of Plant Systems Biology, Vlaams Interuniversitair Instituut voor Biotechnologie, B-9052 Gent, Belgium

[d] Department of Plant Biotechnology and Genetics, Ghent University, B-9052 Gent, Belgium

[e] Oxford Centre for Integrative Systems Biology, Department of Biochemistry, University of Oxford, Oxford OX1 3QU, United Kingdom

[f] Research Center for Eco-environmental Sciences, Chinese Academy of Sciences, Beijing 100085, People's Republic of China

Entry into mitosis is universally controlled by cyclin-dependent kinases (CDKs). A key regulatory event in metazoans and fission yeast is CDK activation by the removal of inhibitory phosphate groups in the ATP binding pocket catalyzed by Cdc25 phosphatases. In contrast with other multicellular organisms, we show here that in the flowering plant *Arabidopsis thaliana*, cell cycle control does not depend on sudden changes in the phosphorylation pattern of the PSTAIRE-containing Cdk1 homolog CDKA;1. Consistently, we found that neither mutants in a previously identified CDC25 candidate gene nor plants in which it is overexpressed display cell cycle defects. Inhibitory phosphorylation of CDKs is also the key event in metazoans to arrest cell cycle progression upon DNA damage. However, we show here that the DNA damage checkpoint in *Arabidopsis* can also operate independently of the phosphorylation of CDKA;1. These observations reveal a surprising degree of divergence in the circuitry of highly conserved core cell cycle regulators in multicellular organisms. Based on biomathematical simulations, we propose a plant-specific model of how progression through the cell cycle could be wired in *Arabidopsis*.

INTRODUCTION

Progression through the eukaryotic cell cycle is governed by cyclin-dependent kinases (CDKs) in conjunction with their cyclin partners (Morgan, 1997). (For nomenclature, *Arabidopsis thaliana* wild-type genes [in italics] and proteins [not italicized] use all uppercase letters, and mutants are in lowercase letters [in italics]. In fission yeast [*Schizosaccharomyces pombe*] and budding yeast [*Saccharomyces cerevisiae*], wild-type proteins are not italicized and in title case, with fission yeast having a postfix superscript "+" and budding yeast a postfix lowercase "p" indicating the protein nature. All other proteins are in title case except if stated otherwise in the National Center for Biotechnology Information [NCBI] library. Generalized terms appear not italicized and uppercase.) A key principle and the driving force of the cell cycle is the generation of alternating phases of high and low kinase activity (Nasmyth, 1996). At times of high CDK-cyclin activity, a number of target proteins become phosphorylated, resulting in DNA synthesis during S phase or the separation of chromosomes during M phase (Ubersax et al., 2003). However, phases of low CDK-cyclin activity, typically the gap phases G1 (before S phase) and G2 (before M phase), are equally important for cell cycle progression.

Inhibition of mammalian Cdk1 by P-loop phosphorylation in G2 phase allows the buildup of inactive CDK-cyclin complexes. Thereby a large momentum is generated that, once a threshold level of these CDK-cyclin complexes is reached, it is rapidly activated, causing a flood of immediately available active CDK. This mechanism functions as an all-or-nothing switch, assuring the irreversible progression into mitosis and, as such, is thought to represent a universal principle of cell cycle control applied in all

[1] Current address: Deutsches Krebsforschungszentrum, Im Neuenheimer Feld 280, D-69120 Heidelberg, Germany.

[2] Current address: Department of Plant Systems Biology, Vlaams Interuniversitair Instituut voor Biotechnologie, Ghent University, Technologiepark 927, B-9052 Gent, Belgium.

[3] Address correspondence to arp.schnittger@ibmp-ulp.u-strasbg.fr.

The authors responsible for distribution of materials integral to the findings presented in this article in accordance with the policy described in the Instructions for Authors (www.plantcell.org) are: Nico Dissmeyer (diss@mpiz-koeln.mpg.de) and Arp Schnittger (arp.schnittger@ibmp-ulp.u-strasbg.fr).

[C]Some figures in this article are displayed in color online but in black and white in the print edition.

[W]Online version contains Web-only data.

www.plantcell.org/cgi/doi/10.1105/tpc.109.070417

organisms having a distinguishable G2 phase (Novak et al., 2001; O'Farrell, 2001).

The inhibitory phosphorylation of the P-loop is catalyzed by Wee1-type and/or Myt1/Mik1$^+$-type kinases. The trigger is then the activation of CDKs by Cdc25, a dual-specificity phosphatase that liberates the CDKs from this inhibitory phosphorylation. Both Wee1 and Cdc25 are linked with CDKs in a positive feedback loop (i.e., active CDKs inhibit Wee1 but activate Cdc25).

As in multicellular organisms, inhibitory phosphorylation also directs the cell cycle in fission yeast (reviewed in Atherton-Fessler et al., 1993). By contrast, in budding yeast, M phase follows immediately after S phase (lacking a G2 phase), and, consistent with the general dogma, phosphorylation control is not used in this organism for entry into mitosis (Amon et al., 1992; Sorger and Murray, 1992; Booher et al., 1993). Nonetheless, inhibitory phosphorylation of Cdc28p is still important in *S. cerevisiae* but as a cell morphogenesis checkpoint.

In *Arabidopsis*, the mitotic cell cycle follows the common scheme of G1, S, G2, and M phases (Inze and Veylder, 2006; Gutierrez, 2008). In particular, the G2 phase is pronounced because cells often exit the cell cycle in this gap phase in plants, indicating an elaborated G2/M checkpoint (Galbraith et al., 1991). The cell cycle machinery is largely conserved in *Arabidopsis*, including the Cdk1 homolog CDKA;1, which contains as the sole CDK in *Arabidopsis* the canonical PSTAIRE amino acid motif required for cyclin binding in Cdk1 or Cdc2$^+$/Cdc28p. CDKA;1 is also up to now the only CDK from *Arabidopsis* that could complement yeast *cdc2*/*cdc28*, while CDKB1;1 (formerly known as Cdc2bAt) was reported to fail so (Ferreira et al., 1991; Hirayama et al., 1991; Imajuku et al., 1992). Mammalian, yeast, and plant PSTAIRE kinases share the key regulatory sites in the T- and P-loops (Dissmeyer et al., 2007; Harashima et al., 2007; see Supplemental Figure 1 online). As shown in other organisms, phosphorylation of the T-loop of the *Arabidopsis* CDKA;1 is required for proper function of this enzyme (Dissmeyer et al., 2007; Harashima et al., 2007). However, phosphorylation of the T-loop is not thought to be regulatory since no indication of a change in phosphorylation state during cell cycle progression was found in *S. cerevisiae* Cdc28p (Hadwiger and Reed, 1988).

Previously, CDKA;1 from *Arabidopsis* and CDKA from tomato (*Solanum lycopersicum*) have been found to be phosphorylated at a Tyr residue in vitro, presumably at the P-loop (Shimotohno et al., 2006; Gonzalez et al., 2007). In addition, although no protein with similarities to Myt1/Mik1$^+$ could be isolated in plants, a Wee1 homolog has been identified in different plant species (Sun et al., 1999; Sorrell et al., 2002; Gonzalez et al., 2004), and in in vitro experiments, WEE1 could phosphorylate CDK and block its activity (Sun et al., 1999; Shimotohno et al., 2006; Gonzalez et al., 2007). RNA interference–mediated downregulation of *WEE1* expression in tomato resulted in reduced plant growth and a smaller fruit size (Gonzalez et al., 2007). By contrast, *wee1* mutants in *Arabidopsis* displayed no growth defects but were susceptible to genotoxic stress consistent with a function of Wee1 at a DNA damage checkpoint in metazoans (De Schutter et al., 2007).

Furthermore, the expression of the *S. pombe* Cdc25$^+$ phosphatase stimulates cell proliferation of a tobacco (*Nicotiana tabacum*) cell culture (*BY-2*) (Orchard et al., 2005), and a potential candidate gene for a CDC25-like phosphatase in *Arabidopsis* was presented (Landrieu et al., 2004).

These findings have suggested that CDKA;1 regulation is conserved between plants and metazoans. However, we show here using dephospho- and phosphomimetic mutants of *CDKA;1*, as well as mutants and overexpression lines of a putative *CDC25* ortholog, that regulatory phosphorylation patterns are strikingly different between *Arabidopsis* and animals or yeasts. These differences are incorporated here into a biomathematical simulation of the plant cell cycle.

RESULTS

The *CDC25* Candidate Gene *At5g03455* Is Not a Key Cell Cycle Regulator in *Arabidopsis*

In metazoans, Cdc25 is one of the most important enzymes in cell cycle control. Exploiting its gatekeeper function for entry into mitosis, Cdc25 also serves as an integrating unit receiving regulatory input from developmental (e.g., growth control) and environmental (e.g., stress sensing) signal transduction cascades. In particular, the large N terminus of Cdc25 has been found to mediate signaling, for instance by harboring phosphorylation sites for the upstream kinases Chk1 and Chk2 (Boutros et al., 2006). However, the presumed CDC25 candidate (encoded by *At5g03455*) in *Arabidopsis* completely lacks a comparable N-terminal regulatory region.

To test whether the CDC25 candidate is important for plant cell cycle control, we isolated a T-DNA insertion mutant that represents a null allele (see Supplemental Figures 2A and 2B online). Unexpectedly, homozygous *cdc25* mutants grew indistinguishably from wild-type plants and, regarding ploidy level, had a similar DNA profile (see Supplemental Figures 2C and 2D online). When quantifying the number of abaxial epidermal cells in leaves, no significant difference was observed between the mutant and control plants (see Supplemental Table 1 online). Conversely, *CDC25* overexpression lines (*CDC25-OE*) also resembled wild-type plants without any indication of overproliferation or increased cell cycle rates (see Supplemental Figures 2C and 2D and Supplemental Table 1 online). The DNA ploidy distribution pattern was also indistinguishable between the different genotypes (see Supplemental Figures 2C and 2D and Supplemental Table 1 online).

Finally, we tested both *cdc25* and *CDC25-OE* for altered behavior on auxin- and cytokinin-containing media because *CDC25* had been proposed to be induced by cytokinin (Suchomelova et al., 2004), but no altered hormone response was observed (see Supplemental Figure 2D online). These results demonstrate that either CDC25 is not involved in cell cycle regulation or, in contrast with yeast and animals, CDC25 is not a rate-limiting component in *Arabidopsis*. Consistent with a function unrelated to the cell cycle, it has recently been found that At5g03455 possesses besides a phosphatase also an arsenate reductase activity (therefore, it was proposed to be named ARSENATE REDUCTASE 2/ArsC-RELATED) and appears to be involved in arsenate metabolism (Bleeker et al., 2006; Ellis et al., 2006). When testing for arsenate reduction, we found that *CDC25-OE*

lines displayed a twofold higher reductase activity in comparison with wild-type plants, while in the extracts from *cdc25* mutant plants, almost no detectable activity levels could be measured, consistent with previously obtained results and supporting the functionality of the here analyzed overexpression lines (see Supplemental Figure 2 online).

Phosphomimicry Version of CDKA;1 Reveals a Conserved Enzymatic Mechanism of PSTAIRE Kinases

Although At5g03455 was the main candidate for an *Arabidopsis* CDC25 homolog, a large class of CDC25-related phosphatases exists that could take over specific subtasks and/or act redundantly in cell cycle control. To complement the above and previously presented data on *cdc25* mutants, we analyzed dephospho- and phosphomimicry versions of CDKA;1 in planta as the most direct and unambiguous way of studying the importance of CDK phosphorylation.

We substituted both conserved phosphorylation sites Thr-14 and Tyr-15 in CDKA;1 with negatively charged Asp and Glu, respectively (in short *DE*; see Supplemental Figures 1 and 3C online). Yellow fluorescent protein fusions of *DE* were stable, displayed the wild-type subcellular localization pattern, and interacted with core cell cycle regulators, such as CYCLIN D3;1, ICK1/KRP1 (for INHIBITOR/INTERACTOR OF CDKs 1/KIP-RELATED-PROTEIN 1), and CKS1 (CDK-SUBUNIT 1), as did wild-type CDKA;1 fusions (see Supplemental Figures 4A and 4B online), illustrating that the introduced mutations did not affect the general behavior of CDKA;1.

Homozygous *cdka;1* mutants that are lethal under greenhouse conditions (Nowack et al., 2006; Iwakawa et al., 2006) can be completely rescued by expressing the *CDKA;1* cDNA under the control of a 2-kb fragment of the presumptive *CDKA;1* promoter region (Nowack et al., 2006). After transformation of the *DE* variant driven by the *CDKA;1* promoter into *cdka;1* heterozygous mutant plants, homozygous *cdka;1* mutant plants could be recovered in the T2 generation that expressed the *DE* variant.

DE plants were severely altered with strongly reduced cell proliferation and growth and only partial rescue of the *cdka;1* mutants (Figures 1A and 1B). The primary phenotype of heterozygous *cdka;1* mutants was a failure to progress through the second mitotic division during male gametophyte development,

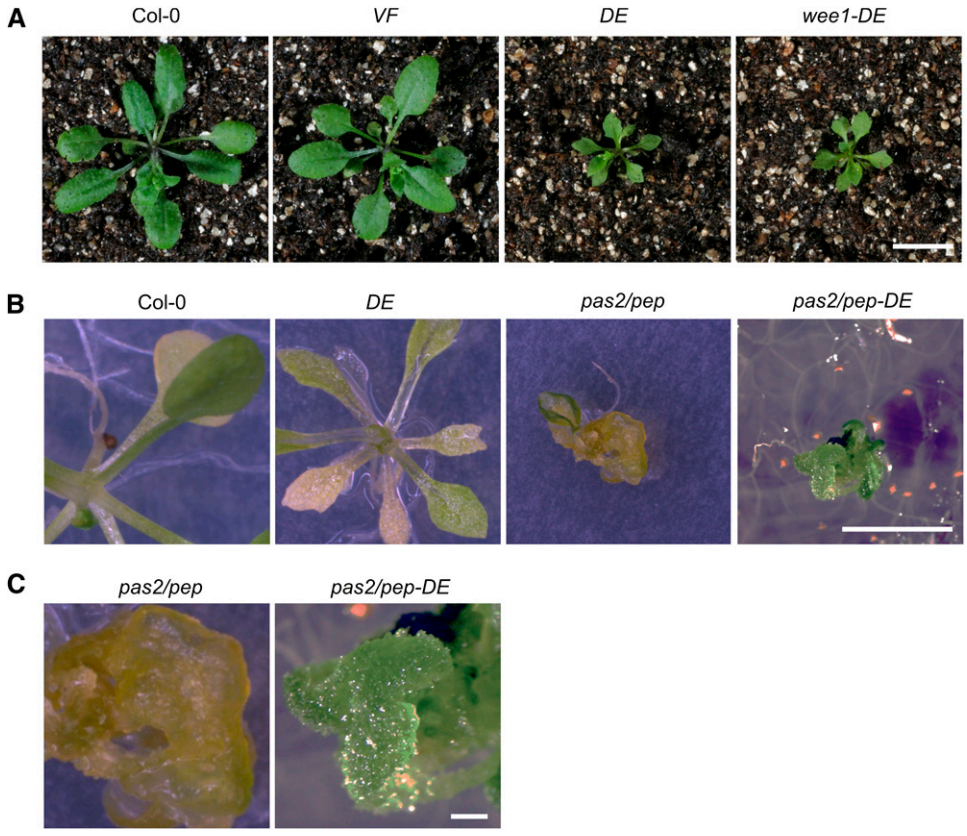

Figure 1. Rosette Morphology of *CDKA;1* Variants and Their Combination with *pas2/pep* and *wee1*.

(A) Strongly reduced growth of 3-week-old *DE* and *wee1-DE* plants in comparison to the wild-type (Columbia-0 [Col-0]) and *VF* plants of the same age.
(B) Characteristic callus-like overproliferation phenotype of 3-week-old *pas2/pep* seedlings grown on agar plates. In the triple mutant *pas2/pep-DE*, the *pas2/pep* phenotype is not restored.
(C) Close-ups of *pas2/pep* and *pas2/pep-DE* from **(B)**.
Bars = 1 cm in **(A)** and **(B)** and 1 mm in **(D)**.

resulting in two-celled pollen containing only one sperm-like cell, in contrast with the normal-looking wild-type pollen with three cells, including two sperms (Iwakawa et al., 2006; Nowack et al., 2006). Testing the extent of a rescue of the gametophytic defects in *DE* plants was not possible since these were completely sterile (data not shown), consistent with previously identified weak *cdka;1* mutant alleles and an observed requirement of CDKA;1 during meiosis (Dissmeyer et al., 2007). Therefore, we analyzed pollen of plants that were homozygous for the *DE* construct and heterozygous for *cdka;1* (Figure 2C). In contrast with heterozygous or homozygous *cdka;1* mutants in which a nonmutated CDKA;1 cDNA is driven from the CDKA;1 promoter, *DE* expressing homozygous *cdka;1* mutants showed between 10 and 30% single sperm pollen (Figure 2D).

Reduced activity of the *DE* variant was also observed when analyzing other plant growth parameters: Roots showed reduced length and a smaller root meristem (see Supplemental Figures 5A, 5C, and 5E online). Root growth rates were less than half those of wild-type plants as determined by kinematic measurements (Figures 3A, 3C, and 3E). Similarly, leaf size was dramatically reduced due to a strong decrease in cell number (Figures 4A to 4C). Consistent with previous observation in plants with reduced CDK activity, we found that the few remaining leaf cells were larger than in the wild type (Figures 4B and 4C).

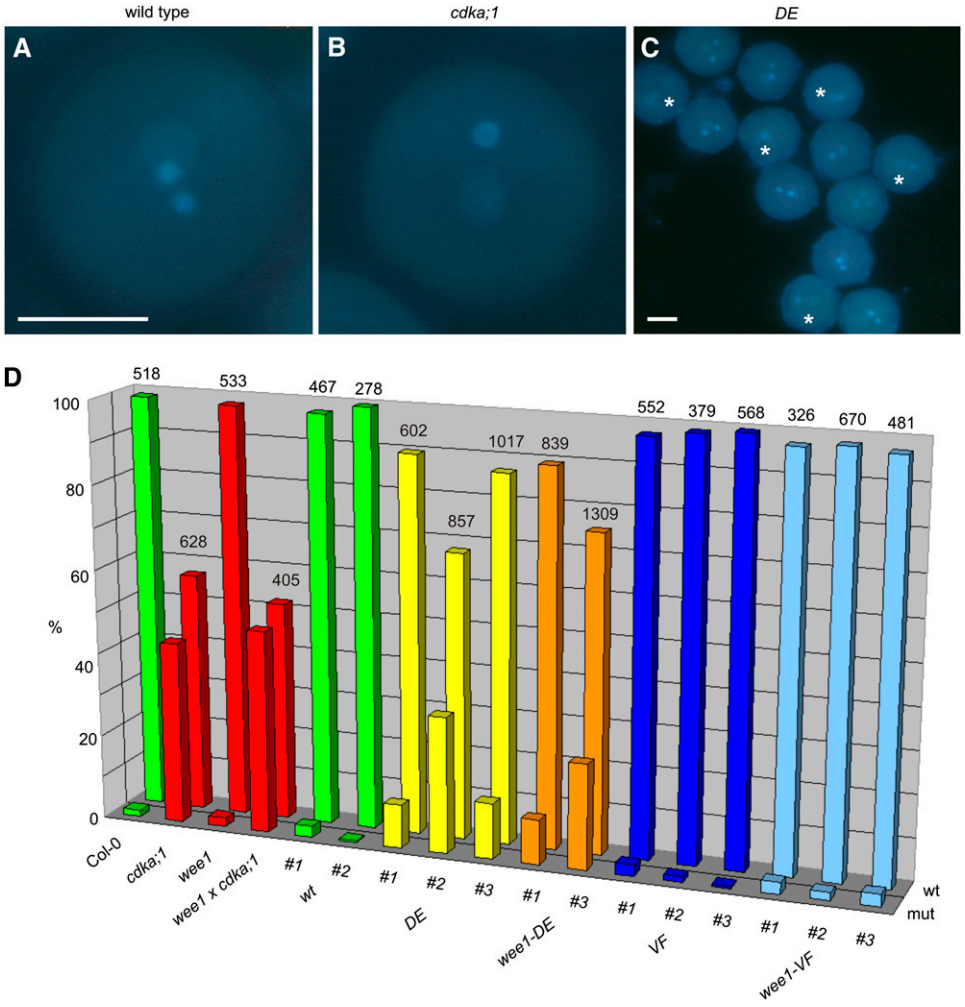

Figure 2. Analysis of Pollen Phenotypes.

(A) to **(C)** DAPI staining of pollen grains. Bars = 10 μm.

(A) Wild-type pollen at anthesis, consisting of three cells: two sperm cells, with two bright and condensed nuclei, embedded in one giant vegetative cell with a large and diffuse nucleus.

(B) Heterozygous *cdka;1* mutants with approximately half of the pollen containing only a single sperm cell-like cell.

(C) In heterozygous *cdka;1* mutants harboring two copies of the *DE* construct, both wild-type and mutant pollen (asterisks) can be found, indicating the reduced activity of *DE*.

(D) Quantification of pollen phenotypes. See Methods for genotype descriptions. The number of pollen scored for each genotype is shown at the top of each graph; *DE* and *wee1-DE* are heterozygous for *cdka;1*. #1, 2, and 3 are individual T3 lines from independent transformation events.

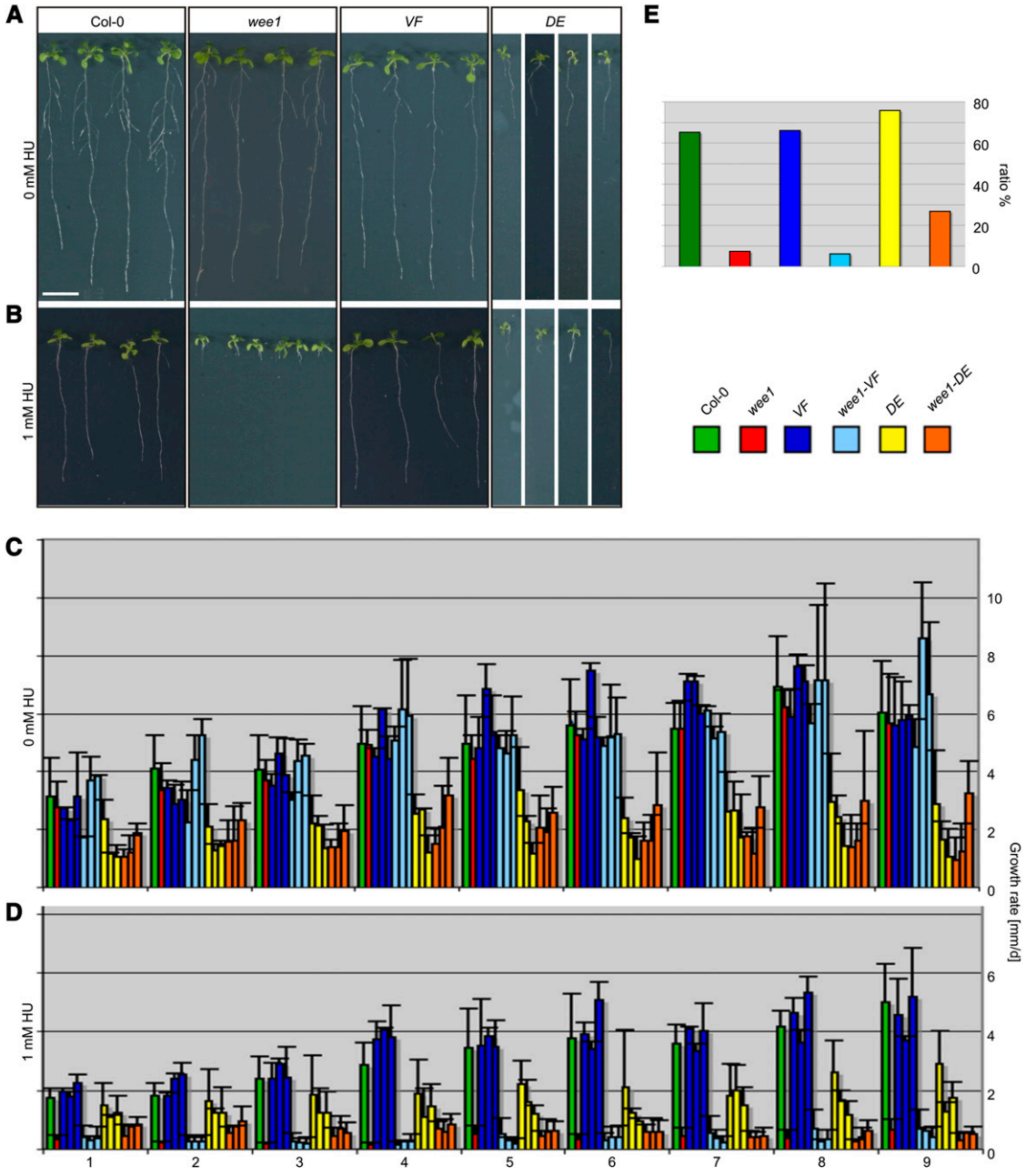

Figure 3. Analysis of Root Growth.

(A) and **(B)** Wild-type (Col-0), *wee1*, *VF*, and *DE* plants were germinated and grown for 10 d **(A)** on Murashige and Skoog (MS) medium **(A)** and on MS medium containing 1 mM HU **(B)**. The *DE* plants were compiled from a segregating population because homozygous *DE* plants are sterile. Bar in **(A)** = 1 cm.

(C) and **(D)** Kinematic analysis of the root growth rate of seedlings grown on MS plates without and with HU for 10 d after germination (abscissa, 1 = growth from day 1 to day 2, etc.). Error bars represent SD of the following data (0 mM HU: replicates/individuals per replicate/1 mM HU: replicates/individuals per replicate): Col-0 (5/49//4/36), *wee1* (5/51//3/31), *VF* #1 (3/30//3/28), *VF* #2 (2/11//2/14), *VF* #3 (3/25//3/24), *DE* #1 (4/34//4/25), *DE* #2 (2/23//2/20), *DE* #3 (4/17//3/18), *wee1-VF* #1 (2/11//2/23), *wee1-VF* #2 (3/33//3/32), *wee1-VF* #3 (3/34//3/29), *wee1-DE* #1 (2/12//3/2), *wee1-DE* #2 (3/16//3/12), and *wee1-DE* #4 (5/35//5/27). Root length was measured from the root tip until the root-hypocotyl border. The mean of the root lengths of each individual experiment was determined and again averaged for the replicates.

(E) Ratio of the mean growth rates on 1 mM HU/0 mM HU of the intervals 4 to 7. The values of the individual sublines #1, #2, and #3 were averaged. Quantification of the final root length after 10 d is shown in Supplemental Figures 3A and 3B online.

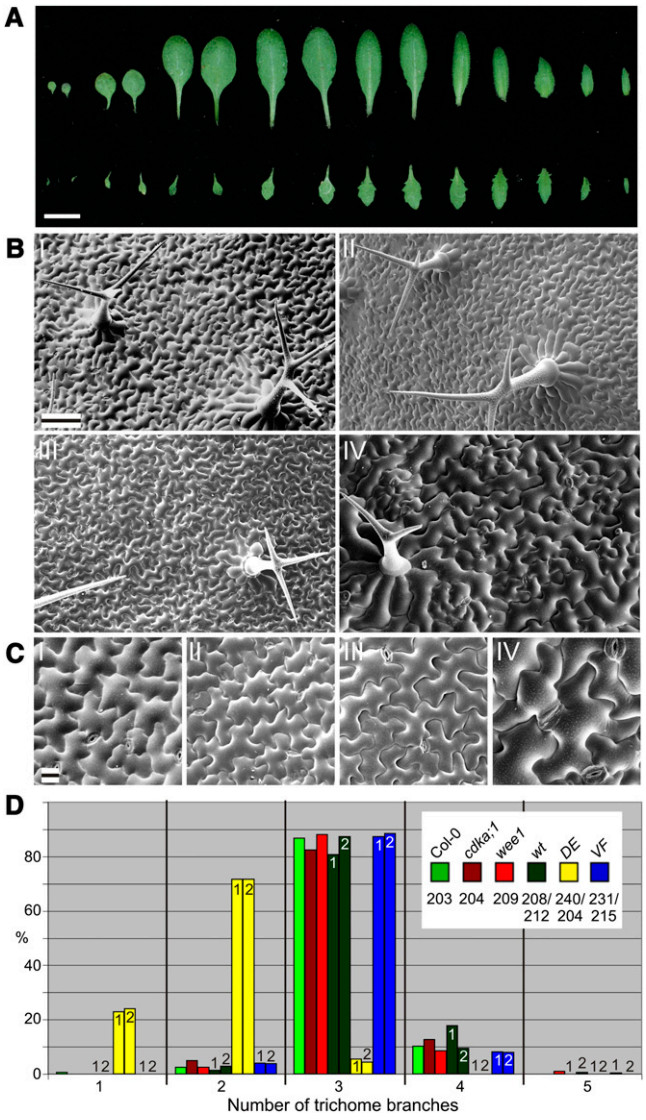

Figure 4. Leaf Morphology and Trichome Branching of *CDKA;1* Variants.

(A) Distinct overall leaf morphology of *DE* (bottom row) from that of wild-type plants (top row). Leaves of *DE* plants are small with a serrated shape; see also Figure 1.

(B) Scanning electron micrographs of leaf surfaces of the same genotypes showing less-branched trichomes (leaf hairs) of *DE* plants (IV) than those of the wild type (I), *wee1* (II), or *VF* (III).

(C) Scanning electron microscopy close-ups of the epidermis of *DE* (IV) that contains fewer but much larger cells than Col-0 (I), *wee1* (II), or *VF* (III).

(D) Quantification of trichome branch numbers. Same genotypes as in Figure 2 unless indicated; number of trichomes scored for each genotype is shown below the color legend (for *wt*, *DE* and *VF*, two individual T3 lines [#1 and #2] from independent transformation events were investigated).

Bars = 1 cm in **(A)**, 20 μm in **(B)**, and 100 μm in **(C)**.

However, cell size was also restricted in *DE* plants as seen by a reduction in the size of trichomes (leaf hairs), which are some of the largest cells in *Arabidopsis* (Figure 4B).

Trichome growth depends on endoreplication, and many cells of *Arabidopsis* wild-type plants undergo cellular polyploidization reaching DNA content levels of up to 32C. Analyses of 4',6-diamidino-2-phenylindole (DAPI)-stained leaves revealed that indeed the nuclear sizes in trichomes as well as most other leaf cells are strongly reduced in *DE* plants (Figures 4C and 5B). Quantification by flow cytometry showed that, in *DE* plants, endoreplication is severely compromised and most of the cells are found in G1 phase with a DNA content of 2C, even at late stages of their development (Figures 5A and 5B).

It is noteworthy that a reduction in cell proliferation and growth was not observed in a wild-type background or in heterozygous *cdka;1* mutants carrying one or two alleles of the *DE* construct. This indicated that *DE* does not function as a dominant negative and that the effect of the *CDKA;1-DE* construct can be overridden by the presence of one wild-type *CDKA;1* allele.

Consistent with the above mutant description, we found dramatically reduced CDKA;1 activity in kinase assays of *DE* plants (Figure 6C). Recently, Tyr-15 phosphorylation of Cdk2 has been shown to result in reduced substrate binding of the kinase (Welburn et al., 2007). Indeed, the interaction of *DE* with a bona fide CDK substrate (i.e., CDC6) was reduced when compared with that of the wild-type CDKA;1 (Figures 7A and 7B).

Taken together, these findings show that CDKA;1 activity is required throughout plant development and underscore that cell proliferation is a major parameter of plant growth.

Dephosphomutants of CDKA;1 Can Fully Substitute for the Wild-Type Kinase without Causing Cell Cycle Defects

The data presented above show that the molecular mechanistics of CDKA;1 are conserved in comparison to other PSTAIRE-CDKs, suggesting the possibility for regulation of CDKA;1 via P-loop phosphorylation in planta. To assess the biological importance of a putative P-loop phosphorylation, we substituted Thr-14 and Tyr-15 with the nonphosphorylatable Ala or Val and Phe, respectively (hereafter abbreviated as *AF* or *VF*; see Supplemental Figures 1 and 3 online). Again, we tested the general parameters of the dephosphovariants and found that their stability and ability to interact with known cofactors were not compromised. In addition, the interaction profile with CDC6 as substrate was the same as that of the wild-type CDKA;1 (Figures 7A and 7B; see Supplemental Figures 4A and 4B online).

In human cells, the expression of a *Cdk1-AF* dephosphomutant pushes cells through the cell cycle and, in particular, forces them into mitotic-like states with only a partially replicated genome (Krek and Nigg, 1991; Pomerening et al., 2008). Similarly, it has been proposed that plants with increased CDKA;1 activity display a callus-like growth with many fast and unorganized proliferating cells (Da Costa et al., 2006). Therefore, we decided to express the dephosphovariants in specific cell types and tissues that would interfere as little as possible with viability and fertility. We chose *Arabidopsis* trichomes as a prototype for cells with an endoreplication cycle and stomata as an example for cells undergoing a mitotic cell cycle. In both cases, the generated transgenic lines

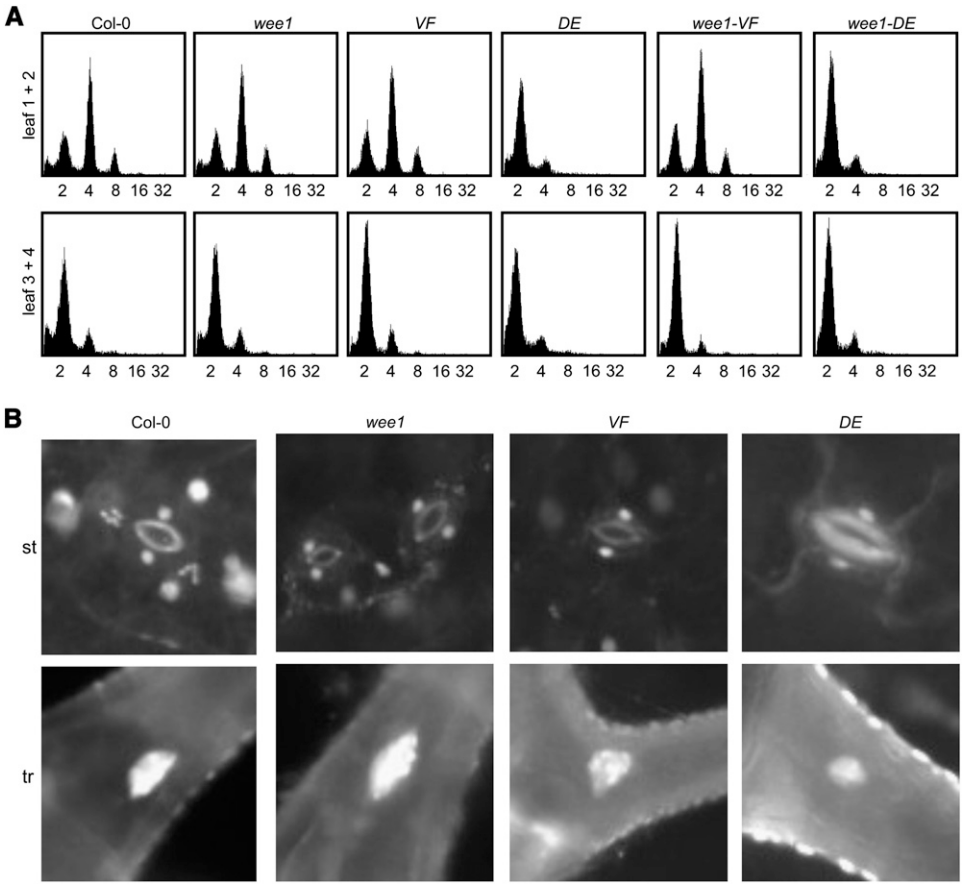

Figure 5. Determination of Ploidy and DNA Content.

(A) Flow cytometry of *Arabidopsis* leaves. For ploidy analysis of each genotype, three independent preparations of pooled leaf material (young [top row, leaves 1 plus 2] and mature [bottom row, leaves 3 plus 4]) of five individuals each were investigated in triplicates. For the transgenics *DE* and *VF* as well as for the combinations *wee1-DE* and *wee1-VF*, three independent transformants (*DE* and *VF* #1, #2, or #3) were investigated homozygous for *cdka;1*. For each profile, 10,000 events were counted. Numbers below the peaks indicate the ploidy (or C-) level.

(B) Details of DAPI-stained leaves in which nuclear morphology and size of stomata (st) in *DE* and *VF* is indistinguishable from those of the wild type, whereas the endoreplication of trichomes (tr) is reduced in *DE*. Individuals were grown under identical conditions for 3 weeks.

expressing this gain-of-function construct were not obviously altered in trichome or stomata morphology (data not shown).

Next, we fused the *CDKA;1-VF* dephosphoversion to the *CDKA;1* promoter and transformed this construct into heterozygous *cdka;1* mutant plants. Surprisingly, *VF* could completely rescue the *cdka;1* mutant phenotype, and the resulting homozygous *cdka;1* mutants expressing the *VF* variant were morphologically indistinguishable from wild-type plants (i.e., in terms of organ and cell size, DNA profile, root growth rates, and, consistent with the above finding, stomata and trichome morphology) (Figures 1A, 2D, 3A, 3C, 4, and 5).

In kinase assays from protein extracts of flower buds, the activity of *VF* was the same as that of the wild-type CDKA;1 (Figure 6). These data illustrate the absence of a G2/M control mechanism by Thr-14 and Tyr-15 phosphorylation for plant PSTAIRE-CDKs under normal growth conditions.

As an alternative or complementary regulatory mechanism to dephosphorylation by CDC25, PASTICCINO2/PEPINO (PAS2/PEP) has been proposed to act on CDKA;1 as an antiphosphatase, protecting the inhibitory phosphate group(s) (Da Costa et al., 2006). However, the wild-type-like phenotype of *VF* plants argues per se against an important role of PAS2/PEP in regulating CDKA;1. To substantiate this finding, we introduced *VF* into *pas2*/*pep* mutants. Homozygous *cdka;1* mutants expressing *VF* in a homozygous *pas2*/*pep* mutant background were indistinguishable from *pas2*/*pep* plants, indicating that *pas2*/*pep-VF* plants still develop a *pas2*/*pep* phenotype (Figures 1B and 1C).

Conversely, we also generated homozygous *cdka;1* mutants expressing the *DE* variant in homozygous *pas2*/*pep* mutants. If the mutant phenotype of *pas2*/*pep* were due to uninhibited CDKA;1, the phenotype of *DE* plants should be epistatic, but the phenotype of *pas2*/*pep-DE* was additive (i.e., plants were tiny, yet overproliferating) (Figures 1B and 1C), corroborating that PAS2/PEP functions in parallel to CDKA;1. Consistent with these observations, it was recently reported that PAS2/PEP is involved in fatty acid metabolism and can function as a 3-hydroxy-acyl-CoA dehydratase (Bach et al., 2008).

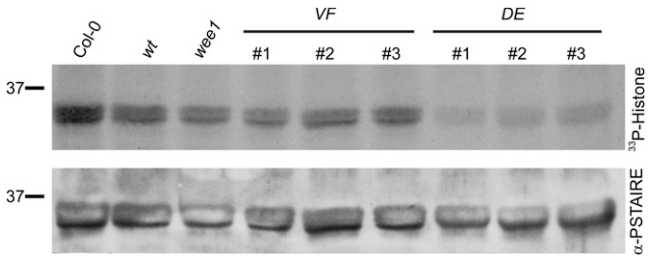

Figure 6. Kinase Activity of *CDKA;1* Variants.

In vitro histone H1 kinase assays of CDKA;1-cyclin complexes from crude extracts of flower buds. [γ-^{33}P] was used as phosphorylation probe. As a loading control, CDKA;1 protein levels were visualized using α-PSTAIRE antibody.

The DNA Damage Response Pathway in *Arabidopsis* Does Not Depend on P-Loop Phosphorylation

P-loop phosphorylation of CDKs was found to be especially crucial in metazoans when the nuclear DNA is damaged (Yata and Esashi, 2009) in order to prevent mitosis of abnormal cells. The previously observed growth defects of the *Arabidopsis wee1* mutant under genotoxic conditions suggested that cells in this mutant cannot delay mitosis to allow DNA repair (De Schutter et al., 2007).

If the *wee1* phenotype on hydroxyurea (HU) was caused by a failure to place the inhibitory phosphorylation marks onto the PSTAIRE kinase only, *VF* plants should completely mimic *wee1* mutants under replication stress conditions. However, kinematic growth assays of *VF* on HU plates indicated that *VF* did not display the *wee1* mutant phenotype but behaved like the wild type (Figures 3B, 3D, and 3E; see Supplemental Figure 5 online).

To validate this observation, we introgressed homozygous *cdka;1* expressing *VF* into homozygous *wee1* mutants (*wee1-VF*). The resulting plants homozygous for all three loci (*cdka;1*, *wee1*, and *VF*) were indistinguishable from wild-type plants under normal growth conditions (Figures 2, 3A, and 3C; see Supplemental Figure 5 online; data not shown). When root growth was analyzed under genotoxic conditions, *wee1-VF* behaved like *wee1* on HU, ruling out that *VF* by itself (as *cdka;1*$^{-/-}$;$_{Pro}$*CDKA;1:CDKA;1-T14V;Y15F*$^{+/+}$) could somehow bypass the requirements for WEE1 under genotoxic stress (Figures 3B, 3D, and 3E; see Supplemental Figure 5 online). Similarly, *CDC25-OE* did not show an increased susceptibility, and the *cdc25* mutant was not more resistant on HU plates than the wild type (see Supplemental Figure 2 online).

Correspondingly, if WEE1 solely operates on CDKA;1, the phosphomimicry *DE* plants should perform on HU-containing media like *wee1-DE*. The triple homozygous mutant *wee1-DE* plants closely resembled *DE* plants (Figures 1A, 2, 3A, 3D, 4, and 5), but *wee1-DE* was still susceptible to HU (Figures 3B, 3D, and 3E).

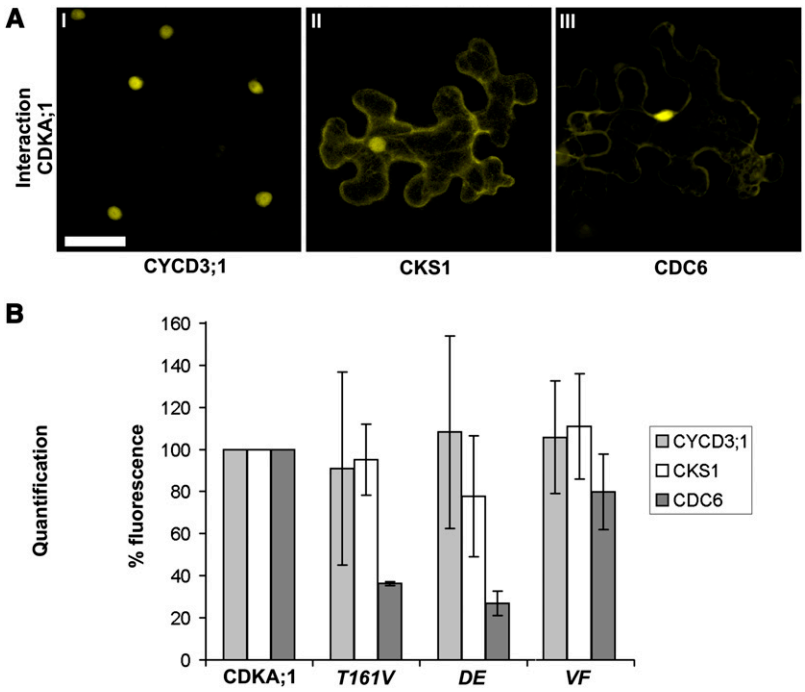

Figure 7. Stability, Localization, and Interaction of *CDKA;1* Variants.

(A) Wild-type CDKA;1 interacts in bimolecular fluorescence complementation assays with nonsubstrate interactors, such as CYCLIN D3;1 (I) or CDK-SUBUNIT 1 (II), and with putative substrates, such as CDC6 (III). Bar = 50 μm.

(B) Quantification of the relative fluorescence intensities. Error bars in the graph indicate SD from at least three independent experiments.

[See online article for color version of this figure.]

Notably, *wee1-DE* plants performed slightly better than *wee1* mutants on HU media, especially during early stages of the HU treatment; thus, a reduction of cell cycle activity might indeed help to grow under replicative stress conditions. However, this effect was small and likely indirect, so we therefore conclude that under genotoxic conditions, *wee1* is epistatic over *DE*, demonstrating that a WEE1-mediated DNA damage response in *Arabidopsis* acts independently of Thr-14 and Tyr-15 phosphorylation.

DISCUSSION

After more than two decades of search for a cell cycle–related Cdc25 homolog in vascular plants, we show here that regulation of the *Arabidopsis* Cdk1 homolog CDKA;1 via dephosphorylation of the P-loop has no biological relevance for plant growth. Similarly, the DNA damage checkpoint is fully functional without phosphorylation of the conserved residues in the P-loop of CDKA;1. At the same time, CDKA;1 kinase activity can be severely compromised by phosphomimetic mutations, likely relying on a similar mechanism as in metazoans (i.e., by affecting substrate binding). This indicates that the kinase mechanistics are conserved between *Arabidopsis*, yeast, and animals, supported by a high degree of sequence similarity between the different species (see Supplemental Figure 1 online) and the fact that *Arabidopsis* CDKA;1 can rescue *cdc2* and *cdc28* mutants in yeast (Ferreira et al., 1991; Hirayama et al., 1991; Imajuku et al., 1992; Porceddu et al., 1999; Dissmeyer et al., 2007). However, the regulatory context and the wiring of Cdk1-like kinases appear to have evolved to be very different in plants.

Control of Mitotic Entry in Plants

The key features of cell cycle progression (i.e., unidirectionality and step-wise progression with the possibility to arrest the cell cycle [checkpoints]) are achieved in animals and yeast by three central oscillating regulatory units that are wired together to achieve stable and alternating states (hysteresis) of CDK activity (Ferrell, 2002; Tyson and Novak, 2008): first, oscillating levels of cyclins, precisely controlled by transcription and protein stability; second, fluctuating levels of CDK inhibitors; and finally, changing states of inhibitory phosphorylation of CDKs. Bistability, the alternation of only two stable steady states (fully active and fully inactive), is reached in this system by various feedback and feed-forward mechanisms. For example, active CDKs phosphorylate and inhibit Wee1 and at the same time activate Cdc25 as shown in *Xenopus laevis* egg cells (Pomerening et al., 2003; Sha et al., 2003).

While it is clear that in plants oscillating levels of cyclins and CKIs (CDK inhibitors) exist that could contribute to CDK bistability (Verkest et al., 2005b; De Veylder et al., 2007), we show here that at least the third major module does not appear to be present in plants. To evaluate the consequences of the absence of this module, we simulated cell cycle progression based on a common cell cycle model (Tyson and Novak, 2001) with and without a CDK-CDC25-WEE1 feedback loop (Figures 8A and 8B). If only non-phosphorylatable CDKA;1 were present, our model predicted stable CDK activity oscillations (Figure 8B), reminiscent of the situation in *S. cerevisiae* in which phosphorylation of the P-loop is not used in cell cycle control. However, similar to *S. cerevisiae*, a G2 phase was virtually eliminated, while *Arabidopsis* and other plants have a defined G2 phase with a clear DNA damage checkpoint (Inze and Veylder, 2006; Gutierrez, 2008).

Based on the above findings, we postulate a plant-specific module that establishes a G2 phase. In theory, entry into mitosis could be controlled by different mechanisms: positive cell cycle regulators that specifically control mitotic targets or negative cell cycle regulators that serve as a relay of CDK activity.

On the side of the positive regulators, two obvious candidates exist that could fulfill this role: The first candidate is additional cyclins. Indeed, one of the key distinctions of the cell cycle repertoire in plants is the enormously increased number of cyclins, with more than 30 cyclins in *Arabidopsis* in comparison to only a handful in yeast or metazoans (Inze and Veylder, 2006). Still very little is known about the different family members, and it remains to be seen whether the diversification in *Arabidopsis* reflects a cell cycle requirement in plants. In our simulations, activation of mitotic cyclin transcription by MPF (M phase promoting factor, called MPF* in our model) could establish a long G2 phase in the absence of a CDK-CDC25-WEE1 loop (Figure 8C). Interestingly, ectopic expression of a tobacco CYCB2 in *BY2* cells was found to push cells into mitosis, indicating that transcriptional regulation of mitotic cyclins is indeed sufficient to modulate the length of G2 phases (Weingartner et al., 2003).

The second candidate is a group of plant-specific B-type CDKs (Boudolf et al., 2006). In particular, the CDKB2 class is expressed in mitosis, and CDKB2s were shown to be important cell cycle regulators in *Arabidopsis* (Andersen et al., 2008). Formally, adding additional CDKs (named CDKX in the model) regulated by cyclin availability (CYCX) or inhibitory phosphorylation could establish a G2 phase in the plant cell cycle (Figure 8C).

Conversely, negative cell cycle regulators could also be involved in establishing a G2 phase, and two classes of CKIs have been identified in *Arabidopsis* up to now: the ICK/KRPs and the SIM/SMRs (SIAMESE/SIM-RELATED PROTEINS; Verkest et al., 2005b; Churchman et al., 2006; Peres et al., 2007). We find with modeling that an MPF-specific CKI (called CKI*) can delay MPF activation and thereby establish a G2 phase of the cell cycle. A key feature of the CKIs in our model is that they should be neither degraded at G1/S nor be substrates of APC/C (anaphase-promoting complex or cyclosome).

However, all ICK/KRPs tested so far in overexpression studies can block both M and S phases (Verkest et al., 2005b), and at least KRP6 and KRP7 appear to be degraded at the G1/S transition point mediated by a CRL (cullin-RING ligase)-FBL17 complex (Kim et al., 2008; Gusti et al., 2009). By contrast, SIM expression appears to be compatible with DNA replication and preferentially represses M phase (Churchman et al., 2006; Peres et al., 2007). Thus, in particular, SIM and the SIM family members could be involved in setting up a plant-specific delay of M phase. Consistent with this is the observation that at least some of the SMRs are expressed in highly proliferating tissues, such as young flower buds and shoot apical meristems (www.bar.utoronto.ca and www.genevestigator.com).

The above models are still not exhaustive since additional, currently cryptic mechanisms could play a role. For example, a feedback loop between CDK activity and transcription factors that in turn activate the transcription of G2/M–specific genes

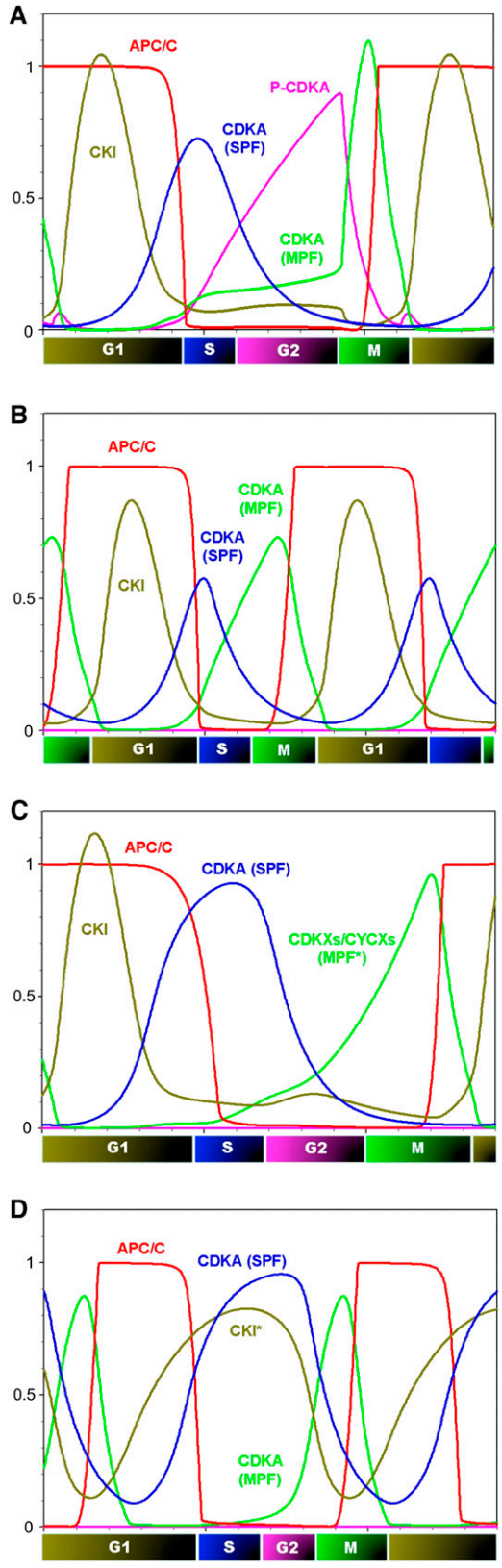

Figure 8. Cell Cycle Simulations.

Numerical simulations are based on a eukaryotic cell cycle model (Tyson and Novak, 2001), and the relative activity levels (0 to 1) of major cell cycle regulators are plotted versus time with the same time window shown in each panel; approximate cell cycle phases are given under each panel.

(A) Cell cycle control with inhibitory phosphorylation of mitosis promoting factor (MPF): S phase and M phase start when the CDKA activities of S phase promoting factor (SPF) and MPF abruptly rise from their low level. The long period between SPF and MPF activation represents the sum of S and G2 phases of the cycle.

(B) Cell cycle control without inhibitory Tyr-15 phosphorylation of MPF: in its absence, MPF activity rises soon after SPF and initiates mitosis prematurely without any G2 phase.

(C) MPF activation with rate-limiting cyclin availability: by assuming that the synthesis (or degradation) of cyclin of MPF (called MPF*) depends on MPF activity, a G2 phase can be established.

(D) MPF regulation by G2 phase–specific CDK inhibitors (CKI*): a stoichiometrically acting CKI can delay MPF activation instead of inhibitory phosphorylations onto CDK-cyclin complexes.

such as B-type cyclins could represent a crucial rely mechanism for cyclin levels as seen for the stabilization of three-repeat Myb in tobacco by CDKA activity (Araki et al., 2004). In addition, special patterns of cyclin destruction can limit cyclin availability (similar to transcription), providing a G2 phase (Figure 8C).

Moreover, given the typical buffering found in biological processes, a combination of different backup scenarios appears likely, such as CKI plus CDKBs or CDKBs plus cyclin availability. Indeed, a link between CDKBs and CKIs has already been found, indicating that ICK2/KRP2 is phosphophorylated by CDKBs and by that marked for degradation, resulting in the liberation of CDKA;1 from the inhibition through ICK2/KRP2 (Verkest et al., 2005a). A combination of special mitotic CDK complexes and CKIs (Figures 8C and 8D) could reinforce a switch-like behavior of CDK activity and accomplish the much faster transition between states of low and high activity (note the difference in the accumulation of MPF activity between Figures 8A versus 8C and 8D).

The Role of WEE1 in the Plant Cell Cycle

Given that the plant cell cycle appears to operate without a CDC25-WEE1 module, what is the role of WEE1 in plants and how can the Tyr phosphorylation patterns on CDKA;1 be explained that has been repeatedly observed?

First of all, the function of WEE1 could be species-specifically adapted as judged from the differences in plant growth between *Arabidopsis wee1* mutants and *WEE1* antisense expression in tomato (De Schutter et al., 2007; Gonzalez et al., 2007). In particular, WEE1 might act in a specific developmental or environmental context analogous to the situation in *S. cerevisiae* where Swe1p (its Wee1 homolog) operates a morphogenesis checkpoint monitoring the integrity of the actin cytoskeleton during bud formation (Lew and Reed, 1995; McMillan et al., 1998). The possibility that Tyr phosphorylation of CDKA;1 is not generally employed during cell proliferation to attenuate kinase activity is supported by recent *Arabidopsis* phosphoproteomics data that documented the phosphorylation of the T- but not of the P-loop of CDKA;1 consistent with previous studies (Dissmeyer

et al., 2007; de la Fuente van Bentem et al., 2008; Sugiyama et al., 2008). However, these are negative data, and caution is required in interpreting the absence of specific phosphopeptides. Moreover, proteome-wide studies clearly do not rule out a context-dependent function of CDK phosphorylation, such as DNA damage or organ-specific functions, such as in fruits (see also below).

Alternatively, WEE1 might target other CDKs than CDKA, for instance, the above-mentioned B-type CDKs, in particular since it is currently often difficult to faithfully discriminate between CDKA and CDKB activities in planta. However, phosphoproteomics data did also not hint at phosphorylated P-loops of any of the CDKBs (de la Fuente van Bentem et al., 2008; Sugiyama et al., 2008). Thus, we propose here that WEE1 is not a core cell cycle regulator but rather functions as a checkpoint kinase similar to the role of the Mik1$^+$ kinase in *S. pombe* but targeting other substrates than a PSTAIRE CDK in *Arabidopsis* (Lundgren et al., 1991; Lee et al., 1994).

At checkpoint conditions, WEE1 might phosphorylate CDKA;1, but its main function could rather be as a stochiometrically acting CKI, for example, by direct binding to CDKs, as suggested by experiments in *S. cerevisiae* where Swe1p inhibits Cdc28p in a nonphosphorylation-dependent manner (McMillan et al., 1999). Thus, one possibility could be that phosphorylation is a byproduct that potentially reinforces the inhibitory binding of WEE1 to CDKA;1 in *Arabidopsis*.

Wee1-like kinases are diversely used in eukaryotes, for example, as a checkpoint kinase versus a mitotic regulator. Therefore, resolving WEE1 function in *Arabidopsis* will also make an important contribution to the understanding of the evolution of cell cycle regulation. This is especially important because it appears that the *Arabidopsis* cell cycle contains components from quite diverse organisms in a unique composition, for example, a distinct G2 phase like in *S. pombe* or metazoans but without a Myt1/Mik1$^+$ and only a single Wee1 homolog, which itself rather functions as a checkpoint-involved Mik1$^+$, yet operating a molecular mechanism that could be more related to Swe1p (Lundgren et al., 1991; Lee et al., 1994). In addition to a different wiring or an altered functional assignment, there are also unique regulators of the plant cell cycle, such as SMRs. To lay the focus on both of these plant cell cycle–specific aspects will be crucial to modulate plant growth in more applied fields, such as breeding energy crops or plants resistant to increasingly harsh environmental conditions, such as high radiation.

METHODS

Plant Material and Growth Conditions

Arabidopsis thaliana plants used in this study were either grown on soil (16 h light; standard mixture consists of eight bags of MiniTray [70 L/bag, Balster Einheitserdewerk]; add 50 liters of water containing 800 mL Osmocote Start [Scotts International] and 250 g BioMükk [Sautter and Stepper]) or in vitro (22 h light; on 0.5% MS medium (Sigma-Aldrich) in Mobylux GroBanks (CLF Plant Climatics). A characterized SALK *cdka;1* T-DNA insertion allele was used (At3g48750, 106809; Nowack et al., 2006), and T-DNA alleles for *wee1* and *cdc25* were isolated from the GABI-Kat collection (*wee1*, At1g02970, 270E05; *cdc25*, At5g03455, 772G06; Li et al., 2007). Seeds heterozygous for the *pas2/pep* (At5g10480) ethyl methanesulfonate alleles pepR254 (old knacki) and pepU306 (alpha) were a generous gift from Ramon Angel Torres Ruiz and are in the Landsberg *erecta* background (Haberer et al., 2002). The *cdka;1* allele can be tracked using the primers ND61/ND62 and wild-type *CDKA;1* with N126/ N127. The *wee1* allele was genotyped with N101/N102, *WEE1* wild type with the latter and N103, with N200/N201, or with N202/N203. The *cdc25* insertion was genotyped with ND97/ N627 and wild-type *CDC25* with N626/N627. Cleaved-amplified polymorphic sequence markers were used to allele-specifically digest PCR products of *pas2/pep*: pepR254, N384/N385/PstI, and pepU306, N382/ N383/BglII.

To determine the root growth rates under genotoxic stress, dry seeds were sterilized with chlorine gas from 75% (v/v) *Eau de Javel* (FLOREAL Haagen) and 25% (v/v) hydrochloric acid, sown on MS supplemented with 1 mM HU (Sigma-Aldrich), elongation of roots marked daily, scanned on a Nashuatec Aficio Docustation DSm730 (RICOH) via Scan-to-Email, and measured with ImageJ (rsb.info.nih.gov/ij).

Transgenic Lines Generated in This Study

The genotypes of the lines used in this work are as follows. T-DNA insertion lines and their crossings: *cdka;1* (*cdka;1*$^{+/-}$; heterozygous T-DNA insertion mutant, background Col-0), *wee1* (*wee1*$^{-/-}$ homozygous T-DNA insertion mutant, background Col-0), *pas2/pep* (*pas2/pep*$^{-/-}$ homozygous T-DNA insertion mutant, background Landsberg *erecta*), and *wee1* × *cdka;1* (*wee1*$^{-/-}$ × *cdka;1*$^{+/-}$).

Transgenic lines: *wt* (rescue; *cdka;1*$^{-/-}$;$_{Pro}$*CDKA;1:CDKA;1*$^{+/+}$), *DE* (phosphomimicry; *cdka;1*$^{-/-}$;$_{Pro}$*CDKA;1:CDKA;1-T14D;Y15E*$^{+/+}$). In addition, to study the gametophytic effect of *DE*, *DE* heterozygous for *cdka;1* were also used: *cdka;1*$^{+/-}$;$_{Pro}$*CDKA;1:CDKA;1-T14D;Y15E*$^{+/+}$, indicated in the text as "*DE* heterozygous for *cdka;1*," *VF* (dephosphomimicry; *cdka;1*$^{-/-}$;$_{Pro}$*CDKA;1:CDKA;1-T14V;Y15F*$^{+/+}$).

Triple mutant lines/crossings of transgenics: *pas2/pep-VF* (*pas2/pep*$^{-/-}$*;cdka;1*$^{-/-}$*;ProCDKA;1-T14V;Y15F*$^{+/+}$), *pas2/pep-DE* (*pas2/pep*$^{-/-}$*;cdka;1*$^{-/-}$;$_{Pro}$*CDKA;1-T14D;Y15E*$^{+/+}$), *wee1-DE* (*wee1*$^{-/-}$*; cdka;1*$^{-/-}$;$_{Pro}$*CDKA;1:CDKA;1-T14D;Y15E*$^{+/+}$). In addition, to study the gametophytic effect of *DE* in this line, plants heterozygous for *cdka;1* were also used: *wee1*$^{-/-}$*;cdka;1*$^{+/-}$;$_{Pro}$*CDKA;1:CDKA;1-T14D; Y15E*$^{+/+}$, indicated in the text as "*wee1-DE* heterozygous for *cdka;1*," *wee1-VF* (*wee1*$^{-/-}$*;cdka;1*$^{-/-}$;$_{Pro}$*CDKA;1:CDKA;1-T14V;Y15F*$^{+/+}$).

DNA Manipulations

Gateway-compatible *Arabidopsis CDKA;1* wild-type cDNA, flanked by attB1 and attB2 sites in *pDONR201* (Invitrogen) was used as the template (plasmid *CK225*, a kind gift of Christina Weinl; Dissmeyer et al., 2007). The phosphorylation site variants of CDKA;1 were generated by site-directed mutagenesis with PfuTurbo (Stratagene) using the primers ND03/ND04 for *DE* and ND01/ND06 and ND51/ND52 for *VF*. The obtained mutated Gateway Entry clones were cloned by Gateway recombination (LR reaction) into the attR site–containing destination vector *pAM-PAT-GW-ProCDKA;1* that carries phosphinothricin-*N*-acetyltransferase (Nowack et al., 2006). The resulting binary plant expression vector, which confers phosphinotricine (BASTA; Bayer Cropscience) resistance, was retransformed into *Agrobacterium tumefaciens GV3101-pMP90RK* (Koncz and Schell, 1986). The *CDC25* overexpression construct (*CDC25-OE*) was generated by the isolation of the full-length coding sequence of *CDC25* from *Arabidopsis* seedling cDNA by PCR using N624/N625, followed by subcloning into *pDONR201*. The PCR fragment was then recombined into *pK7WG2D* (LR) under the control of the cauliflower mosaic virus 35S promoter. The construction of bimolecular fluorescence complementation (BiFC) vectors was described previously (Jakoby et al., 2006). All primer sequences are listed in Supplemental Table 2 online.

Plant Transformation and Selection

Heterozygous *cdka;1* plants were transformed by a modified version of the floral dip method (Clough and Bent, 1998). Standard lines were established by isolating T3 plants homozygous for the transgene. For crosses between mutants and transgenic lines, both *cdka;1* homozygous (*VF*) or heterozygous (*DE*) T3 plants had to be used, and from the following generations, again, lines homozygous for the constructs were identified and used for further experiments. At least 20 transgenic plants were generated for all expression constructs. A number of representative reference lines displaying a typical phenotype were chosen for further analysis.

Kinase Assays

Flowers were processed for kinase assays as described previously (Dissmeyer et al., 2007) with one deviation: $p13^{Suc1}$-agarose beads (Millipore) and stabilized [γ-^{33}P]ATP at >6000 Ci/mmol (Hartmann Analytic). After wet blotting, the CDKA;1 loading was probed with a 1:1000 dilution of rabbit α-PSTAIRE (Santa Cruz Biotechnology) and 1:5000 HRP-conjugated goat anti-rabbit (ImmunoPure; Pierce). Enhanced chemoluminescent detection was performed with SuperSignal West Pico substrate (Pierce).

BiFC Assays

The assay on leaves of tobacco (*Nicotiana benthamiana*) was performed as previously described (Jakoby et al., 2006). The *Agrobacterium* strains containing the BiFC vectors were infiltrated on the abaxial leaf side of 2-month-old tobacco plants and analyzed after 3 to 5 d via confocal microscopy.

Histology

For fluorescence microscopy of leaf nuclei, whole leaves were fixed in 4% formaldehyde in PBT (phosphate-buffered saline/Tween, 140 mM NaCl, 2.7 mM KCl, 10 mM Na_2HPO_4, 1.8 mM KH_2PO_4 to pH 7.2 with HCl, contains 0.1% Tween 20) at 4°C overnight, washed twice with PBT, infiltrated with DAPI staining solution (5 μg/mL DAPI and 5% DMSO in PBT at pH 7.2) under vacuum for 30 min, and incubated at 4°C overnight. DAPI staining of pollen was done as described previously (Dissmeyer et al., 2007). For root cell wall staining, entire 5-d-old seedlings were mounted directly in a saturated solution of propidium iodide in tap water and incubated for 5 min.

Flow Cytometry

Rosette leaves were chopped with razor blades in CyStain UV-precise P buffers, filtered through a 50-μm nylon mesh, and analyzed with a Ploidy Analyzer PA-1 (all materials from Partec). Data were analyzed with FloMax 2.52 (Partec). For *cdc25* and *CDC25-OE*, leaves and cotyledons were frozen in liquid nitrogen, and DNA content was measured as described (De Schutter et al., 2007).

Microscopy

Light microscopy was performed with an Axiophot microscope (Zeiss) and confocal laser scanning microscopy with a TCS SP2 AOBS CLSM system (Leica Microsystems). Photographs of in vitro cultures were taken with a KY-F70 digital camera (JVC) mounted onto a MZ FLIII fluorescence stereomicroscope (Leica). The DISKUS software package (version 4.30.242; Technisches Büro Carl H. Hilgers) was used for documentation. Scanning electron microscopy was done with a SUPRA 40VP (Zeiss) equipped with a K1250X Cryogenic SEM Preparation System (EMITECH) at the on-campus microscopy core facility Zentrale Mikroskopie (CeMic).

Cell Cycle Model Simulations

A general eukaryotic cell cycle model was used for numerical simulations (Tyson and Novak, 2001). The model centers around two CDK-cyclin complexes responsible for initiation of S (SPF) and M phase (MPF). MPF activity is controlled by regulated cyclin degradation through APC/C, by stoichiometric CKIs and reversible inhibitory phosphorylation/dephosphorylation reactions catalyzed by Wee1 and Cdc25-like. All of these processes are regulated by MPF, which establishes important regulatory feedback loops in the molecular mechanisms. G1 phase is terminated by autocatalytic activation of SPF, which also inactivates APC/C and promotes the degradation of the CKIs. However, active MPF inhibits the transcription of the SPF cyclin component and thereby downregulates SPF activity. In the original model (Tyson and Novak, 2001), cell size has an effect on cell cycle progression, which has been omitted in this case for simplicity. Numerical simulations were performed by XPPAUT (www.math.pitt.edu/~bard/xpp/xpp.html).

Accession Numbers

Sequence data from this article can be found at The Arabidopsis Information Resource (TAIR; www.Arabidopsis.org) and the NCBI (www.ncbi.nlm.nih.gov) under the following accession numbers. For TAIR, At3g48750 (At CDKA;1), At1g02970 (At WEE1), At5g03455 (At CDC25), At5g10480 (At PAS/PEP); for NCBI, GenBank AP008208.1 (Os_ CDKA-2), GenBank CAD56245.1 (Pp Cdk-A), GeneID 176374 (Ce_Cdk-1), GeneID 34411 (Dm Cdc2), GeneID 396252 (Gg CDC2), GeneID 983 (Hs Cdk1), GeneID 12534 (Mm Cdc2), GeneID 54237 (Rn Cdc2), GenBank CAA43807.1 (Hs Cdk2), GeneID 852457 (Sc CDC28), GenBank AAP94021.1 (Um Cdk1), GeneID 2539869 (Sp $Cdc2^{+}$). Germplasm information for deposited T-DNA-lines is as follows: *cdka;1* (SALK_106809/Germplasm 4824368), *wee1* (GABI_270E05/Germplasm 3510610662), and *cdc25* (GABI_772G06/Germplasm 3510654948).

Author Contributions

A.S. and N.D. designed the research, and N.D. performed and analyzed most of the experiments. A.K.W. performed the root growth analysis. S.P. conducted the BiFC work and the transient protein localization studies in tobacco. K.D.S. and C.L.A.K. functionally characterized At5g03455 (CDC25) under supervision of L.D.V. M.K.N. analyzed the pollen phenotypes, and B.N. contributed the cell cycle models. G.-L.D. and Y.-G.Z. performed arsenate reduction experiments. A.S. and N.D. wrote the manuscript with contributions from the coauthors. All authors discussed the results and commented on the manuscript.

Supplemental Data

The following materials are available in the online version of this article.

Supplemental Figure 1. P-Loop Alignment of PSTAIRE Kinases.

Supplemental Figure 2. Molecular Analysis of *Arabidopsis* CDC25-Like.

Supplemental Figure 3. Transgene Verification.

Supplemental Figure 4. Subcellular Localization of *CDKA;1* Variants.

Supplemental Figure 5. Root Growth and Morphology.

Supplemental Table 1. Size and Number of Abaxial Pavement Cells in First Leaves of *cdc25*, *CDC25-OE*, and Wild-Type Plants.

Supplemental Table 2. Oligonucleotides Used in This Study.

Supplemental Methods.

Supplemental References.

ACKNOWLEDGMENTS

We thank Jonathan Bramsiepe for help in describing trichome phenotypes, Elmon Schmelzer and Rolf-Dieter Hirtz for microscopy, and MAret-Linda KAlda for photographical documentation. We thank Andreas Lautscham and Monika Bürgel for their excellent support in the greenhouse facilities. We are grateful to Timo Aichler, Toon Cools, Martine De Cock, Hirofumi Harashima, Masami Sekine, and Masaaki Umeda for critical reading and helpful comments on the manuscript. This work was supported by grants from the Volkswagen-Stiftung, an Action Thématique et Incitative sur Programme grant from the Centre National de la Recherche Scientifique to A.S., and the Interuniversity Attraction Poles Programme (IUAP VI/33) to L.D.V., initiated by the Belgian Science Policy Office. N.D. is a fellow of the International Max Planck Research School and funded by the Max Planck Society. L.D.V. is a postdoctoral fellow of the Research Foundation-Flanders.

Received August 11, 2009; revised September 24, 2009; accepted October 22, 2009; published November 30, 2009.

REFERENCES

Amon, A., Surana, U., Muroff, I., and Nasmyth, K. (1992). Regulation of p34CDC28 tyrosine phosphorylation is not required for entry into mitosis in *S. cerevisiae*. Nature **355:** 368–371.

Andersen, S.U., Buechel, S., Zhao, Z., Ljung, K., Novak, O., Busch, W., Schuster, C., and Lohmann, J.U. (2008). Requirement of B2-type cyclin-dependent kinases for meristem integrity in *Arabidopsis thaliana*. Plant Cell **20:** 88–100.

Araki, S., Ito, M., Soyano, T., Nishihama, R., and Machida, Y. (2004). Mitotic cyclins stimulate the activity of c-Myb-like factors for transactivation of G2/M phase-specific genes in tobacco. J. Biol. Chem. **279:** 32979–32988.

Atherton-Fessler, S., Parker, L.L., Geahlen, R.L., and Piwnica-Worms, H. (1993). Mechanisms of p34cdc2 regulation. Mol. Cell. Biol. **13:** 1675–1685.

Bach, L., et al. (2008). The very-long-chain hydroxy fatty acyl-CoA dehydratase PASTICCINO2 is essential and limiting for plant development. Proc. Natl. Acad. Sci. USA **105:** 14727–14731.

Bleeker, P.M., Hakvoort, H.W., Bliek, M., Souer, E., and Schat, H. (2006). Enhanced arsenate reduction by a CDC25-like tyrosine phosphatase explains increased phytochelatin accumulation in arsenate-tolerant *Holcus lanatus*. Plant J. **45:** 917–929.

Booher, R.N., Deshaies, R.J., and Kirschner, M.W. (1993). Properties of *Saccharomyces cerevisiae* wee1 and its differential regulation of p34CDC28 in response to G1 and G2 cyclins. EMBO J. **12:** 3417–3426.

Boudolf, V., Inzé, D., and De Veylder, L. (2006). What if higher plants lack a CDC25 phosphatase? Trends Plant Sci. **11:** 474–479.

Boutros, R., Dozier, C., and Ducommun, B. (2006). The when and wheres of CDC25 phosphatases. Curr. Opin. Cell Biol. **18:** 185–191.

Churchman, M.L., et al. (2006). SIAMESE, a plant-specific cell cycle regulator, controls endoreplication onset in *Arabidopsis thaliana*. Plant Cell **18:** 3145–3157.

Clough, S.J., and Bent, A.F. (1998). Floral dip: A simplified method for Agrobacterium-mediated transformation of *Arabidopsis thaliana.* Plant J. **16:** 735–743.

Da Costa, M., Bach, L., Landrieu, I., Bellec, Y., Catrice, O., Brown, S., De Veylder, L., Lippens, G., Inze, D., and Faure, J.D. (2006). *Arabidopsis* PASTICCINO2 is an antiphosphatase involved in regulation of cyclin-dependent kinase A. Plant Cell **18:** 1426–1437.

de la Fuente van Bentem, S., et al. (2008). Site-specific phosphorylation profiling of Arabidopsis proteins by mass spectrometry and peptide chip analysis. J. Proteome Res. **7:** 2458–2470.

De Schutter, K., Joubes, J., Cools, T., Verkest, A., Corellou, F., Babiychuk, E., Van Der Schueren, E., Beeckman, T., Kushnir, S., Inze, D., and De Veylder, L. (2007). *Arabidopsis* WEE1 kinase controls cell cycle arrest in response to activation of the DNA integrity checkpoint. Plant Cell **19:** 211–225.

De Veylder, L., Beeckman, T., and Inze, D. (2007). The ins and outs of the plant cell cycle. Nat. Rev. Mol. Cell Biol. **8:** 655–665.

Dissmeyer, N., Nowack, M.K., Pusch, S., Stals, H., Inze, D., Grini, P. E., and Schnittger, A. (2007). T-loop phosphorylation of *Arabidopsis* CDKA;1 is required for its function and can be partially substituted by an aspartate residue. Plant Cell **19:** 972–985.

Ellis, D.R., Gumaelius, L., Indriolo, E., Pickering, I.J., Banks, J.A., and Salt, D.E. (2006). A novel arsenate reductase from the arsenic hyperaccumulating fern *Pteris vittata*. Plant Physiol. **141:** 1544–1554.

Ferreira, P.C., Hemerly, A.S., Villarroel, R., Van Montagu, M., and Inze, D. (1991). The *Arabidopsis* functional homolog of the p34cdc2 protein kinase. Plant Cell **3:** 531–540.

Ferrell, J. (2002). Self-perpetuating states in signal transduction: Positive feedback, double-negative feedback and bistability. Curr. Opin. Cell Biol. **14:** 140–148.

Galbraith, D.W., Harkins, K.R., and Knapp, S. (1991). Systemic endopolyploidy in *Arabidopsis thaliana*. Plant Physiol. **96:** 985–989.

Gonzalez, N., Gevaudant, F., Hernould, M., Chevalier, C., and Mouras, A. (2007). The cell cycle-associated protein kinase WEE1 regulates cell size in relation to endoreduplication in developing tomato fruit. Plant J. **51:** 642–655.

Gonzalez, N., Hernould, M., Delmas, F., Gevaudant, F., Duffe, P., Causse, M., Mouras, A., and Chevalier, C. (2004). Molecular characterization of a WEE1 gene homologue in tomato (*Lycopersicon esculentum* Mill.). Plant Mol. Biol. **56:** 849–861.

Gusti, A., Baumberger, N., Nowack, M., Pusch, S., Eisler, H., Potuschak, T., De Veylder, L., Schnittger, A., and Genschik, P. (2009). The *Arabidopsis thaliana* F-box protein FBL17 is essential for progression through the second mitosis during pollen development. PLoS One **4:** e4780.

Gutierrez, C. (2008). The Arabidopsis cell division cycle. In The Arabidopsis Book, R. Last, C. Chang, G. Jander, D. Kliebenstein, R. McClung, and H. Millar, eds (Rockville, MD: American Society of Plant Biologists), pp. 1–19.

Haberer, G., Erschadi, S., and Torres-Ruiz, R.A. (2002). The Arabidopsis gene PEPINO/PASTICCINO2 is required for proliferation control of meristematic and non-meristematic cells and encodes a putative anti-phosphatase. Dev. Genes Evol. **212:** 542–550.

Hadwiger, J.A., and Reed, S.I. (1988). Invariant phosphorylation of the *Saccharomyces cerevisiae* Cdc28 protein kinase. Mol. Cell. Biol. **8:** 2976–2979.

Harashima, H., Shinmyo, A., and Sekine, M. (2007). Phosphorylation of threonine 161 in plant cyclin-dependent kinase A is required for cell division by activation of its associated kinase. Plant J. **52:** 435–448.

Hirayama, T., Imajuku, Y., Anai, T., Matsui, M., and Oka, A. (1991). Identification of two cell-cycle-controlling cdc2 gene homologs in *Arabidopsis thaliana*. Gene **105:** 159–165.

Imajuku, Y., Hirayama, T., Endoh, H., and Oka, A. (1992). Exon-intron organization of the Arabidopsis thaliana protein kinase genes CDC2a and CDC2b. FEBS Lett. **304:** 73–77.

Inze, D., and Veylder, L.D. (2006). Cell cycle regulation in plant development. Annu. Rev. Genet. **40:** 77–105.

Iwakawa, H., Shinmyo, A., and Sekine, M. (2006). Arabidopsis CDKA;1, a cdc2 homologue, controls proliferation of generative cells in male gametogenesis. Plant J. **45:** 819–831.

Jakoby, M.J., Weinl, C., Pusch, S., Kuijt, S.J., Merkle, T., Dissmeyer,

N., and Schnittger, A. (2006). Analysis of the subcellular localization, function and proteolytic control of the Arabidopsis CDK inhibitor ICK1/KRP1. Plant Physiol. **141:** 1293–1305.

Kim, H.J., Oh, S.A., Brownfield, L., Hong, S.H., Ryu, H., Hwang, I., Twell, D., and Nam, H.G. (2008). Control of plant germline proliferation by SCF(FBL17) degradation of cell cycle inhibitors. Nature **455:** 1134–1137.

Koncz, C., and Schell, J. (1986). The promotor of $T_{L\text{-}DNA}$ gene 5 controls the tissue-specific expression of chimaeric genes carried by a noval Agrobacterium binary vector. Mol. Gen. Genet. **204:** 383–396.

Krek, W., and Nigg, E.A. (1991). Mutations of p34cdc2 phosphorylation sites induce premature mitotic events in HeLa cells: Evidence for a double block to p34cdc2 kinase activation in vertebrates. EMBO J. **10:** 3331–3341.

Landrieu, I., da Costa, M., De Veylder, L., Dewitte, F., Vandepoele, K., Hassan, S., Wieruszeski, J.M., Corellou, F., Faure, J.D., Van Montagu, M., Inze, D., and Lippens, G. (2004). A small CDC25 dual-specificity tyrosine-phosphatase isoform in *Arabidopsis thaliana*. Proc. Natl. Acad. Sci. USA **101:** 13380–13385.

Lee, M.S., Enoch, T., and Piwnica-Worms, H. (1994). mik1+ encodes a tyrosine kinase that phosphorylates p34cdc2 on tyrosine 15. J. Biol. Chem. **269:** 30530–30537.

Lew, D.J., and Reed, S.I. (1995). A cell cycle checkpoint monitors cell morphogenesis in budding yeast. J. Cell Biol. **129:** 739–749.

Li, Y., Rosso, M.G., Viehoever, P., and Weisshaar, B. (2007). GABI-Kat SimpleSearch: An *Arabidopsis thaliana* T-DNA mutant database with detailed information for confirmed insertions. Nucleic Acids Res. **35:** D874–D878.

Lundgren, K., Walworth, N., Booher, R., Dembski, M., Kirschner, M., and Beach, D. (1991). mik1 and wee1 cooperate in the inhibitory tyrosine phosphorylation of cdc2. Cell **64:** 1111–1122.

McMillan, J.N., Sia, R.A., Bardes, E.S., and Lew, D.J. (1999). Phosphorylation-independent inhibition of Cdc28p by the tyrosine kinase Swe1p in the morphogenesis checkpoint. Mol. Cell. Biol. **19:** 5981–5990.

McMillan, J.N., Sia, R.A., and Lew, D.J. (1998). A morphogenesis checkpoint monitors the actin cytoskeleton in yeast. J. Cell Biol. **142:** 1487–1499.

Morgan, D.O. (1997). Cyclin-dependent kinases: Engines, clocks, and microprocessors. Annu. Rev. Cell Dev. Biol. **13:** 261–291.

Nasmyth, K. (1996). At the heart of the budding yeast cell cycle. Trends Genet. **12:** 405–412.

Novak, B., Pataki, Z., Ciliberto, A., and Tyson, J.J. (2001). Mathematical model of the cell division cycle of fission yeast. Chaos **11:** 277–286.

Nowack, M.K., Grini, P.E., Jakoby, M.J., Lafos, M., Koncz, C., and Schnittger, A. (2006). A positive signal from the fertilization of the egg cell sets off endosperm proliferation in angiosperm embryogenesis. Nat. Genet. **38:** 63–67.

O'Farrell, P.H. (2001). Triggering the all-or-nothing switch into mitosis. Trends Cell Biol. **11:** 512–519.

Orchard, C.B., Siciliano, I., Sorrell, D.A., Marchbank, A., Rogers, H. J., Francis, D., Herbert, R.J., Suchomelova, P., Lipavska, H., Azmi, A., and Van Onckelen, H. (2005). Tobacco BY-2 cells expressing fission yeast cdc25 bypass a G2/M block on the cell cycle. Plant J. **44:** 290–299.

Peres, A., et al. (2007). Novel plant-specific cyclin-dependent kinase inhibitors induced by biotic and abiotic stresses. J. Biol. Chem. **282:** 25588–25596.

Pomerening, J.R., Sontag, E.D., and Ferrell, J.E., Jr. (2003). Building a cell cycle oscillator: Hysteresis and bistability in the activation of Cdc2. Nat. Cell Biol. **5:** 346–351.

Pomerening, J.R., Ubersax, J.A., and Ferrell, J.E.J. (2008). Rapid cycling and precocious termination of G1 phase in cells expressing CDK1AF. Mol. Biol. Cell **19:** 3426–3441.

Porceddu, A., De Veylder, L., Hayles, J., Van Montagu, M., Inze, D., and Mironov, V. (1999). Mutational analysis of two *Arabidopsis thaliana* cyclin-dependent kinases in fission yeast. FEBS Lett. **446:** 182–188.

Sha, W., Moore, J., Chen, K., Lassaletta, A.D., Yi, C.S., Tyson, J.J., and Sible, J.C. (2003). Hysteresis drives cell-cycle transitions in *Xenopus laevis* egg extracts. Proc. Natl. Acad. Sci. USA **100:** 975–980.

Shimotohno, A., Ohno, R., Bisova, K., Sakaguchi, N., Huang, J., Koncz, C., Uchimiya, H., and Umeda, M. (2006). Diverse phosphoregulatory mechanisms controlling cyclin-dependent kinase-activating kinases in Arabidopsis. Plant J. **47:** 701–710.

Sorger, P.K., and Murray, A.W. (1992). S-phase feedback control in budding yeast independent of tyrosine phosphorylation of p34cdc28. Nature **355:** 365–368.

Sorrell, D.A., Marchbank, A., McMahon, K., Dickinson, J.R., Rogers, H.J., and Francis, D. (2002). A WEE1 homologue from *Arabidopsis thaliana*. Planta **215:** 518–522.

Suchomelova, P., Velgova, D., Masek, T., Francis, D., Rogers, H.J., Marchbank, A.M., and Lipavska, H. (2004). Expression of the fission yeast cell cycle regulator cdc25 induces de novo shoot formation in tobacco: Evidence of a cytokinin-like effect by this mitotic activator. Plant Physiol. Biochem. **42:** 49–55.

Sugiyama, N., Nakagami, H., Mochida, K., Daudi, A., Tomita, M., Shirasu, K., and Ishihama, Y. (2008). Large-scale phosphorylation mapping reveals the extent of tyrosine phosphorylation in Arabidopsis. Mol. Syst. Biol. **4:** 193.

Sun, Y., Dilkes, B.P., Zhang, C., Dante, R.A., Carneiro, N.P., Lowe, K. S., Jung, R., Gordon-Kamm, W.J., and Larkins, B.A. (1999). Characterization of maize (*Zea mays* L.) Wee1 and its activity in developing endosperm. Proc. Natl. Acad. Sci. USA **96:** 4180–4185.

Tyson, J.J., and Novak, B. (2001). Regulation of the eukaryotic cell cycle: molecular antagonism, hysteresis, and irreversible transitions. J. Theor. Biol. **210:** 249–263.

Tyson, J.J., and Novak, B. (2008). Temporal organization of the cell cycle. Curr. Biol. **18:** R759–R768.

Ubersax, J.A., Woodbury, E.L., Quang, P.N., Paraz, M., Blethrow, J. D., Shah, K., Shokat, K.M., and Morgan, D.O. (2003). Targets of the cyclin-dependent kinase Cdk1. Nature **425:** 859–864.

Verkest, A., Manes, C.L., Vercruysse, S., Maes, S., Van Der Schueren, E., Beeckman, T., Genschik, P., Kuiper, M., Inze, D., and De Veylder, L. (2005a). The cyclin-dependent kinase inhibitor KRP2 controls the onset of the endoreduplication cycle during *Arabidopsis* leaf development through inhibition of mitotic CDKA;1 kinase complexes. Plant Cell **17:** 1723–1736.

Verkest, A., Weinl, C., Inze, D., De Veylder, L., and Schnittger, A. (2005b). Switching the cell cycle. Kip-related proteins in plant cell cycle control. Plant Physiol. **139:** 1099–1106.

Weingartner, M., Pelayo, H.R., Binarova, P., Zwerger, K., Melikant, B., de la Torre, C., Heberle-Bors, E., and Bögre, L. (2003). A plant cyclin B2 is degraded early in mitosis and its ectopic expression shortens G2-phase and alleviates the DNA-damage checkpoint. J. Cell Sci. **116:** 487–498.

Welburn, J.P., Tucker, J.A., Johnson, T., Lindert, L., Morgan, M., Willis, A., Noble, M.E., and Endicott, J.A. (2007). How tyrosine 15 phosphorylation inhibits the activity of cyclin-dependent kinase 2-cyclin A. J. Biol. Chem. **282:** 3173–3181.

Yata, K., and Esashi, F. (2009). Dual role of CDKs in DNA repair: To be, or not to be. DNA Repair (Amst.) **8:** 6–18.